



Adsorption and kinetic studies of piperidin-1-yl-phosphonic acid as a corrosion inhibitor of iron in sulphuric acid medium

M. R. Laamari^{a*}, J. benzakour^a, F. Berrekhis^b, M. Bakasse^c, D. Villemin^d

^a *Laboratoire Physico-chimie des Matériaux et Environnement, Université Cadi Ayyad, Faculté des Sciences Semlalia, BP 2390, Marrakech, Morocco*

^b *Laboratoire de Chimie Physique, Ecole Normale Supérieure, BP 2400, Marrakech, Morocco.*

^c *Laboratoire de Chimie Organique, Biorganique et Environnement, Université Chouaib Doukkali, Faculté des Sciences, El Jadida, Morocco.*

^d *École Nationale Supérieure d'Ingénieurs de Caen UMR 6507 CNRS, Bd Maréchal Juin 14050 Caen Cedex, France*

Received 4 Nov 2011, Revised 22 Jan 2012, Accepted 22 Jan 2012.

Corresponding Author: Email: r.laamari@ucam.ac.ma, Fax: (+212) 5 24 62 70 26

Abstract

The inhibitive effect of the piperidin-1-yl-phosphonic acid (PPA) on the corrosion of iron in 0.5 M H₂SO₄ solution has been investigated by weight loss measurement, potentiodynamic polarization and electrochemical impedance spectroscopy (EIS) techniques. The presence of (PPA) reduces remarkably the corrosion rate of iron in acidic solution. The effect of temperature on the corrosion behavior of iron was studied in the range of 298–328 K. Our results clearly reveal that the (PPA) behaves as a mixed type corrosion inhibitor with the highest inhibition at 5 mM. The adsorption of PPA on the iron surface obeys to the Langmuir's adsorption isotherm.

Key words: iron; thermodynamic parameters; phosphonic acid; inhibition.

1. Introduction

The use of inhibitors is one of the most practical methods for metals protection against corrosion in acidic media [1]. Acidic solutions are used extensively in chemical and several industrial processes such as acid pickling, acid cleaning, acid descaling and oil wet cleaning among others uses [2]. Chemical inhibitors are often used for these processes mainly to control the metal dissolution and acid consumption. Most of well-known acid corrosion inhibitors are organic compounds containing nitrogen, sulfur or oxygen atoms [3–7]. It has been found that most of the organic inhibitors act by adsorption on the metal surface [8]. This phenomenon is influenced by the nature and surface charge of metal, the type of aggressive electrolyte and the chemical structure of inhibitors [9]. A large number of organic compounds were studied as corrosion inhibitors for iron and low alloyed steels [10-12]. Most of them are toxic in nature. This has led to the development of non-toxic corrosion inhibitors such as tryptamine [13], cefazolin [14], mebendazole [15,16], 2,3-diphenylbenzoquinoline [17].

Phosphonates, which were originally introduced as scale inhibitors in water treatment, were later proved to be good corrosion inhibitors also [18]. Their impact on environment was reported to be negligible at the concentration levels used for corrosion inhibition [19-20]. There are excellent sequestering agents for electroplating, chemical plating, degreasing and cleaning [21]. The use of phosphonic acids for the protection of iron and its alloys from corrosion in different media has been the subject of several researcher works [22-30].

In this contribution, we report on our attempt to use electrochemical impedance spectroscopy (EIS), potentiodynamic polarization, weight loss, and scanning electron microscopy (SEM) to investigate the nature of adsorption of PPA on iron surface.

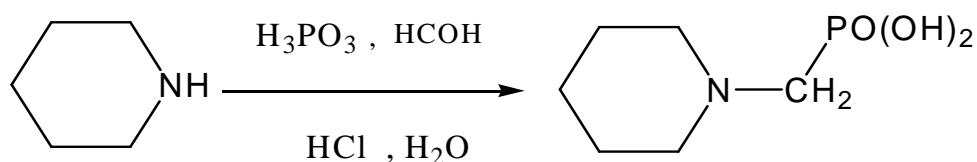
2. Experimental

2.1. Electrochemical cell

Electrochemical experiments were performed using a conventional three electrode cell assembly. The working electrode is An Armco iron rotating disk with surface area of 1 cm^2 and had the following composition (O: 0.03%, Mn: 0.03%, N: 0.018%, S: 0.018%, C: 0.012%, P: 0.004%, Fe: 99.8%). It is abraded with different emery papers up to 1200 grade, washed thoroughly with double-distilled water, degreased with AR grade ethanol, acetone and drying at room temperature.

A saturated calomel electrode (SCE) was used as the reference electrode. All the measured potentials presented in the experimental work are referred to this electrode. The counter electrode was a platinum plate with a surface area of 2 cm^2 .

The organic compound tested is piperidin-1-yl-phosphonic acid (PPA). It is synthesized by the microwave (mono-mode Prolabo Synthewave 402) technique by the following reaction:



The obtained product was purified and characterized using ^1H , ^{13}C , ^{31}P nuclear magnetic resonance (Fourier BrukerAC250 multinuclear) and infra-red spectroscopic (Pekin Elmer 16 PC FT-IR spectrometer) methods [27]. The molecular structure of the studied phosphonic acid compound is shown Fig. 1.

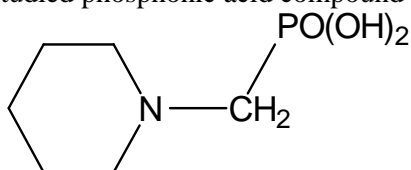


Figure 1 Structure of Piperidin-1-yl-phosphonic acid (PPA)

The aggressive solutions, $0.5 \text{ M H}_2\text{SO}_4$ were prepared by dilution of analytical grade 98% H_2SO_4 with distilled water. The inhibitor is added to freshly prepared $0.5 \text{ M H}_2\text{SO}_4$ in the concentration range of $0.1 - 5 \text{ mM}$.

2.2. Methods

2.2.1. Gravimetric measurements

Gravimetric measurements were carried out in a double walled glass cell equipped with a thermostat-cooling condenser. The solution volume was 100 mL of $0.5 \text{ M H}_2\text{SO}_4$ with and without addition of different concentrations of inhibitor. The iron specimens used have a rectangular form ($2 \text{ cm} \times 2 \text{ cm} \times 0.05 \text{ cm}$). The immersion time for the weight loss was 24 h at 298 K and 6 h at the other temperatures. After the corrosion test, the specimens of iron were carefully washed in double-distilled water, dried and then weighed. The rinse removed loose segments of the film of the corroded samples. Triplicate experiments were performed in each case and the mean value of the weight loss is reported. Weight loss allowed us to calculate the mean corrosion rate as expressed in $\text{mg cm}^{-2} \text{ h}^{-1}$. The inhibition efficiency (IE %) was determined by using the following equation:

$$IE\% = \frac{CR_0 - CR}{CR_0} \times 100 \quad (1)$$

Where, CR and CR_0 are the corrosion rates of iron with and without the inhibitor, respectively.

2.2.2. Electrochemical measurements

Two electrochemical techniques, namely DC-Tafel slope and AC-electrochemical impedance spectroscopy (EIS), were used to study the corrosion behaviour. All experiments were performed in one-compartment cell with three electrodes connected to a Voltalab 10 (Radiometer PGZ 100) system controlled by the Volta master 4 corrosion analysis software model.

Polarisation curves were obtained by changing the electrode potential automatically from -800 to -300 mV versus open circuit potential (E_{ocp}) at a scan rate of 1 mVs^{-1} . The inhibition efficiency is calculated by the following equation:

$$IE\% = \frac{i_{corr}^0 - i_{corr}}{i_{corr}^0} \times 100 \quad (2)$$

Where i_{corr}^0 and i_{corr} are the corrosion current density values without and with inhibitor, respectively.

EIS measurements were carried out under potentiostatic conditions in the frequency range $100 - 0.01$ Hz, with amplitude of 10 mV peak-to-peak, using AC signal at E_{ocp} . All experiments were performed after immersion for 60 min in $0.5 \text{ M H}_2\text{SO}_4$ with and without addition of inhibitor.

2.2.3. Surface morphology

For morphological study, surface features ($0.9 \times 0.8 \times 0.2$ cm) of Armco iron were examined after exposure to $0.5 \text{ M H}_2\text{SO}_4$ solution after 1 day with and without inhibitor. JEOL JSM-5500 scanning electron microscope was used for this investigation.

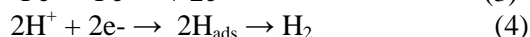
3. Results and discussion

3.1. Weight loss measurements

3.1.1. Effect of inhibitor concentration

Corrosion inhibition performance of organic compounds as corrosion inhibitors can be evaluated using electrochemical and chemical techniques. For the chemical methods, a weight loss measurement is ideally suited for long term immersion test. Corroborative results between weight loss and other techniques have been already reported [31–34].

The anodic dissolution of iron in acidic media and the corresponding cathodic reaction has been reported to proceed as follows [35]:



As a result of these reactions, including the high solubility of the corrosion products, the metal loses weight in the solution. The values of corrosion rate and inhibition efficiency from gravimetric measurements at different concentrations of PPA are summarized in Table 1, and the inhibition efficiency as a function of concentration is shown in Fig. 2. The results show that as the inhibitor concentration increases, the corrosion rate decreases and therefore the inhibition efficiency increases. It can be concluded that this inhibitor acts through adsorption on iron surface and formation of a barrier layer between the metal and the corrosive media.

Table 1 Corrosion parameters obtained from weight loss measurements for iron in $0.5 \text{ M H}_2\text{SO}_4$ containing various concentrations of PPA at 298 K .

C (M)	CR ($\text{mg cm}^{-2} \text{ h}^{-1}$)	IE %
Blank	0.43	-
0.0001	0.24	44
0.0005	0.14	67
0.001	0.10	77
0.005	0.02	95

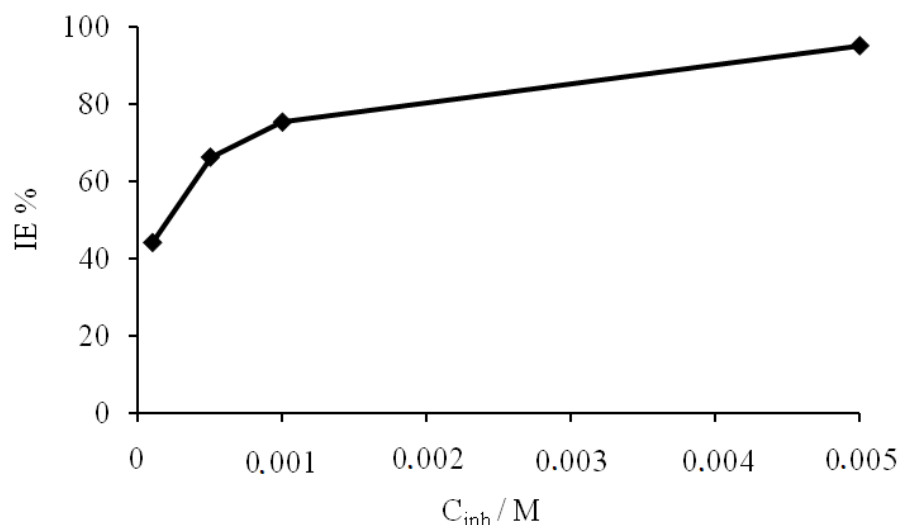


Figure 2 Variation of inhibition efficiency (IE%) with the concentration of PPA for iron in 0.5 M H₂SO₄

3.1.2. Effects of temperature

Temperature has a great effect on the rate of metal electrochemical corrosion. In case of corrosion in an acidic medium the corrosion rate increases exponentially with temperature increase because the hydrogen evolution over potential decreases [36]. Furthermore, the value of inhibition efficiency indicates the adsorption ability of inhibitor molecules on the metal surface; the higher inhibition efficiency results in the higher adsorption [37]. The effect of temperature on the adsorption behavior of PPA was investigated using weight loss measurements in the temperature range of 298–328 K with and without inhibitor at different concentrations in 0.5 M H₂SO₄. The values of inhibition efficiency obtained are given in Table 2 and Fig. 3. It is clear that inhibition efficiency increased as far as inhibitor concentration increases. The maximum value of inhibition efficiency (IE%) obtained for 5 mM PPA is 95% at 298 K. The inhibition efficiencies decrease slightly with increasing temperature, indicating that higher temperature dissolution of iron predominates on adsorption of PPA at the metal surface.

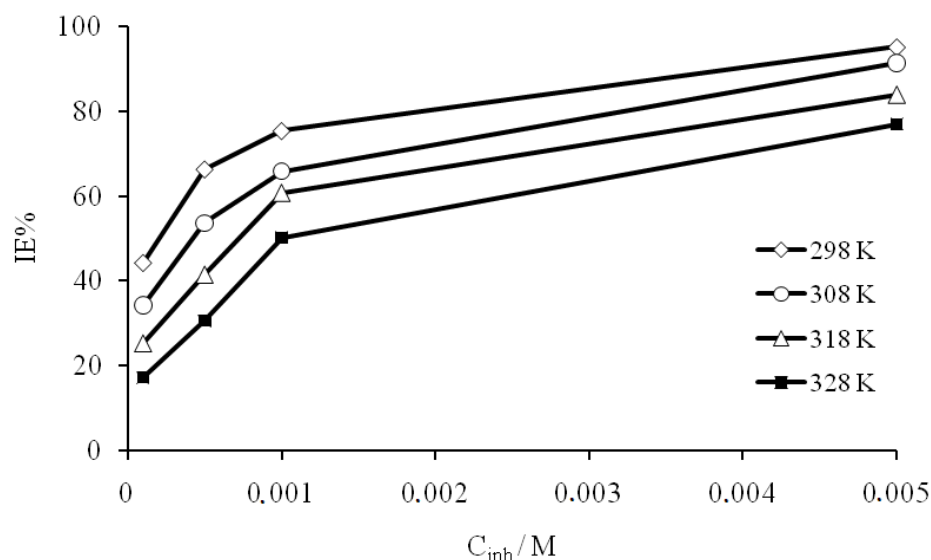


Figure 3 Variation of inhibition efficiency (IE%) with concentration of PPA for iron in 0.5 M H₂SO₄ at different temperatures.

In order to obtain more details on the corrosion process, activation kinetic parameters such activation energy (E_a); enthalpy (ΔH°) and entropy (ΔS°) are obtained from the effect of temperature using Arrhenius law (Eq. (5)) and the alternative formulation of Arrhenius equation (Eq. (6)) [12,14]:

$$\log(CR) = \log A - \frac{E_a}{2.303RT} \quad (5)$$

$$CR = \left(\frac{RT}{Nh}\right) \exp\left(\frac{\Delta S^\circ}{R}\right) \exp\left(-\frac{\Delta H^\circ}{RT}\right) \quad (6)$$

where CR is the corrosion rate, R is the universal gas constant, T is the absolute temperature, A is the pre-exponential factor, h is Plank's constant and N is Avogadro's number.

The plot of $\log CR$ against $1/T$ for iron corrosion in 0.5M H_2SO_4 in the absence and presence of different concentrations of PPA is presented in Fig.4. All parameters are given in Table 3. In the present study, it could be seen that the activation energy was higher in the presence of inhibitor compared with the blank. In addition, increasing concentration of PPA results in the increasing of the activation energy. Such increase of the activation energies in the presence of inhibitor is attributed to an appreciable decrease in the adsorption process of the inhibitor on the metal surface with increase in temperature; and corresponding increase in the reaction rate because of the greater area of the metal exposed to acid [38]. A decrease in inhibition efficiency upon rising the temperature, with analogous increase in corrosion activation energy in the presence of inhibitor compared to its absence, is a good evidence for physisorption mechanism of PPA on the iron surface [38-40].

Table 2 Corrosion parameters obtained from weight loss for iron in 0.5 M H_2SO_4 containing various concentrations of PPA at different temperatures.

C (M)	CR (mg.cm ⁻² .h ⁻¹)				IE %			
	298	308	318	328	298	308	318	328
Blank	0.43	0.82	1.30	2.25	-	-	-	-
0.0005	0.241	0.54	0.97	1.86	44	34	25	17
0.001	0.145	0.38	0.76	1.56	66	53	41	30
0.002	0.106	0.28	0.51	1.12	75	66	60	50
0.004	0.021	0.07	0.21	0.52	95	91	84	77

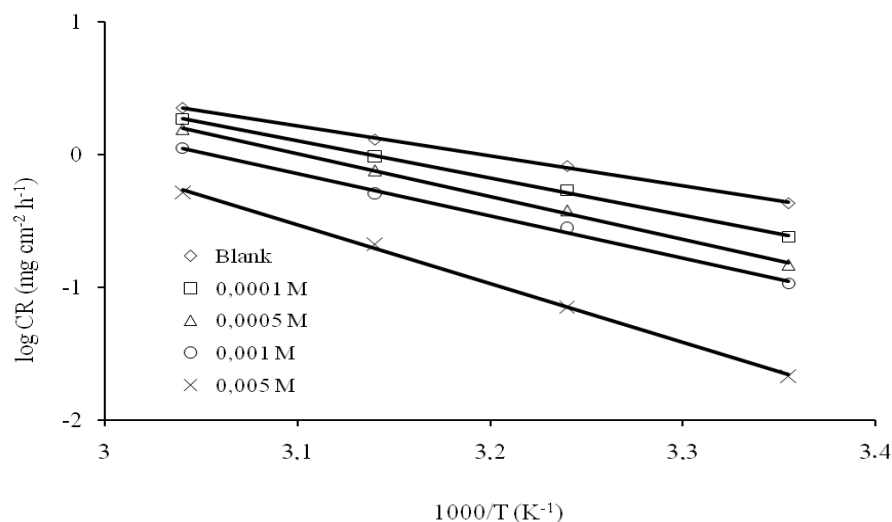


Figure 4 Arrhenius plots for iron corrosion rates (CR) in 0.5 M H_2SO_4 with and without different concentrations of PPA.

Experimental corrosion rate values obtained from weight loss measurements was used to further gain insight on the change of enthalpy (ΔH°) and entropy (ΔS°) of activation for the formation of the activation complex in the transition state using equation (Eq. (6)).

Fig. 5 shows the plot of $\log(CR/T)$ versus $1/T$ for iron corrosion in 0.5 M H_2SO_4 in the absence and presence of different concentrations of PPA. Straight lines were obtained with slope of $(\Delta H^\circ/2.303R)$ and an intercept of $[\log(R/Nh) (\Delta S^\circ/2.303R)]$ from which the values of ΔH° and ΔS° respectively were computed and listed also in Table 3. The positive signs of ΔH° reflect the endothermic nature of the iron dissolution process [41]. By comparing the values of entropy of activation ΔS° , it is clear that entropy of activation increased in presence of the studied inhibitor compared to free acid solution. Such variation is associated with the phenomenon of ordering and disordering of inhibitor molecules on the iron surface. The increased entropy of activation in the presence of inhibitor indicated that disorderness is increased on going from reactant to activated complex [42]. Therefore, the decrease in corrosion rate is mostly decided by higher values of E_a and ΔH° since both parameters increases with concentration resulting in the reduction of the corrosion rate of iron. The results obtained are in agreement with Eq. (5) and (6) which indicate that higher E_a and ΔH° lead to lower corrosion rate.

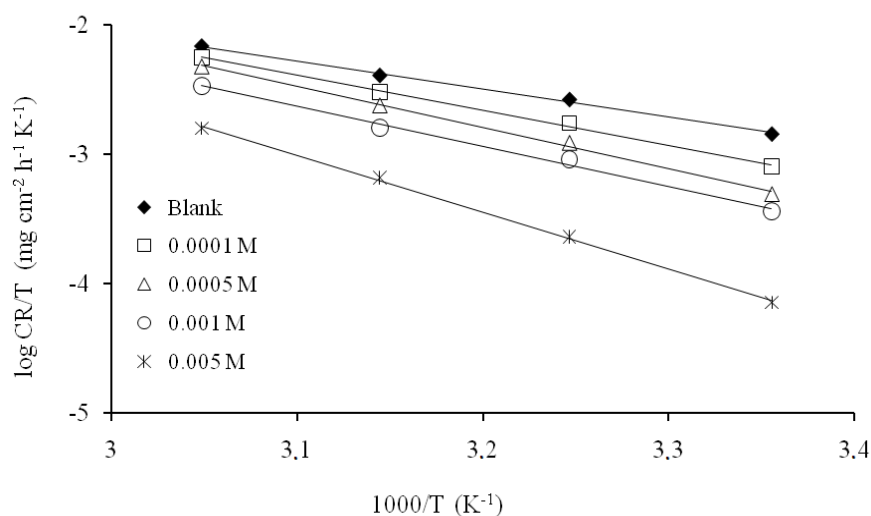


Figure 5 Transition-state plots for iron corrosion rates (CR) in 0.5 M H_2SO_4 with and without different concentrations of PPA.

Table 3 Corrosion kinetic parameters for iron in 0.5 M H_2SO_4 at different concentrations of PPA.

C_{inh} (M)	E_a (kJ mol ⁻¹)	R	ΔH° (kJ mol ⁻¹)	ΔS° (J mol ⁻¹)
Blank	41.11	0.998	41.48	-112.75
0.0005	50.07	0.998	51.92	-81.89
0.001	57.3	0.996	60.6	-63.37
0.002	61.06	0.998	59.57	-57.29
0.004	83.08	0.998	84.11	5.97

3.3. Adsorption isotherm

Adsorption depends mainly on the charge and nature of the metal surface, electronic characteristics of the metal surface, adsorption of solvent and other ionic species, temperature of corrosion reaction and on the electrochemical potential at solution-interface. Adsorption of inhibitor involves the formation of two types of interaction responsible for bonding of inhibitor to a metal surface. The first one (physical adsorption) is weak undirected interaction and is due to electrostatic attraction between inhibiting organic ions or dipoles and the electrically charged surface of metal. The second type of interaction (Chemical adsorption) occurs when directed forces govern the interaction between the adsorbate and adsorbent. Chemical adsorption involves charge sharing or charge transfer from the adsorbate to the metal surface atoms in order to form a coordinative type of bond. Chemical adsorption has a free energy of adsorption and activation energy higher than physical adsorption and, hence, usually it is irreversible [43]. Adsorption isotherms are very important in determining the mechanism of organic electrochemical reactions. Several adsorption isotherms can be

used to assess the adsorption behavior of the inhibitors. The most frequently used are Langmuir, Temkin and Frumkin. In order to obtain the adsorption isotherm, the degree of surface coverage (θ) for various concentrations of the inhibitor has been calculated according to the equation:

$$\theta = \frac{CR_0 - CR}{CR_0} \quad (7)$$

Where, CR and CR_0 are the corrosion rates of iron with and without the inhibitor, respectively. Langmuir isotherm was tested for its fit to the experimental data. Langmuir isotherm is given by following equation:

$$\frac{C_{inh}}{\theta} = \frac{1}{K_{ads}} + C_{inh} \quad (8)$$

where θ is the surface coverage, C_{inh} is the molar concentration of inhibitor and K_{ads} is the equilibrium constant of the adsorption process.

From the values of surface coverage, the linear regressions between $\frac{C_{inh}}{\theta}$ and C_{inh} are calculated and the parameters are listed in Table 4. Fig. 6 shows the relationship between $\frac{C_{inh}}{\theta}$ and C_{inh} at various temperatures. These results show that the linear regression coefficients (R) are almost close to 1.000, indicating that the adsorption of inhibitor onto iron surface agrees to the Langmuir adsorption isotherm.

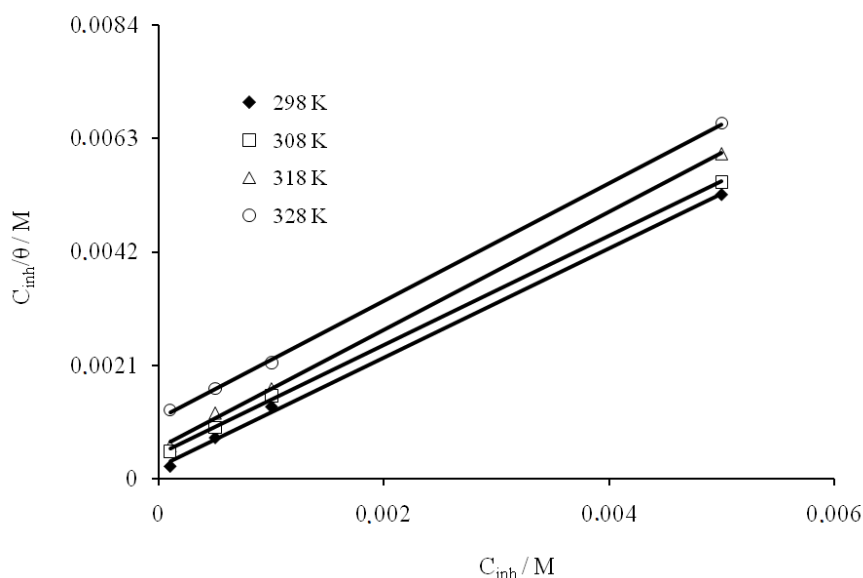


Figure 6 Langmuir's isotherm adsorption model of PPA on the iron surface in 0.5 M H_2SO_4 at different temperatures.

Table 4 Thermodynamic parameters for the adsorption of PPA on the iron in 0.5 M H_2SO_4 at different temperatures.

Temperature (K)	R^2	K_{ads}	ΔG°_{ads} (kJ mol $^{-1}$)
298	0.998	5×10^3	-31.08
308	0.999	2×10^3	-29.77
318	0.999	1.66×10^3	-30.26
328	0.999	1×10^3	-29.18

The equilibrium constants of the adsorption process (K_{ads}) decrease upon increasing the temperature values (Table 4). It is well known that K_{ads} indicates the adsorption power of the inhibitor onto the metal

surface. Clearly, PPA gives higher values of K_{ads} at lower temperatures, indicating that it was adsorbed strongly onto the iron surface. Thus, the inhibition efficiency decreased slightly with the increase in temperature as the result of the improvement of desorption of PPA from the metal surface. The standard adsorption free energy (ΔG°_{ads}) is obtained according to the following equation:

$$\Delta G^{\circ}_{ads} = -2.303RT \log(55.5K_{ads}) \quad (9)$$

where R is the universal gas constant, T the thermodynamic temperature and the value 55.5 is the molar concentration of water in the solution.

The large values of ΔG°_{ads} and its negative sign are usually characteristic of a strong interaction and a high efficient adsorption [44]. Generally, values of ΔG°_{ads} up to -20 kJ mol^{-1} are consistent with physisorption while those around -40 kJ mol^{-1} or higher are associated with chemisorption as a result of sharing or transferring of electrons from organic molecules to the metal surface to form a coordinate type of bond [39-41]. In the present study, the calculated values of ΔG°_{ads} obtained for PPA range between -29.18 and $-31.08 \text{ kJ mol}^{-1}$ (Table 4), indicating that the adsorption mechanism of PPA on iron in $0.5 \text{ M H}_2\text{SO}_4$ solution at the studied temperatures may be a combination of both physisorption and chemisorption (comprehensive adsorption) [30,45].

3.3. Potentiodynamic polarization studies

The potentiodynamic polarization behavior of iron in $0.5 \text{ M H}_2\text{SO}_4$ with the addition of various concentrations of PPA inhibitor is shown in Fig.7. The corrosion kinetic parameters such as corrosion potential (E_{corr}), corrosion current density (I_{corr}), anodic and cathodic Tafel slopes (b_a and b_c) were derived from these curves and given in Table 5.

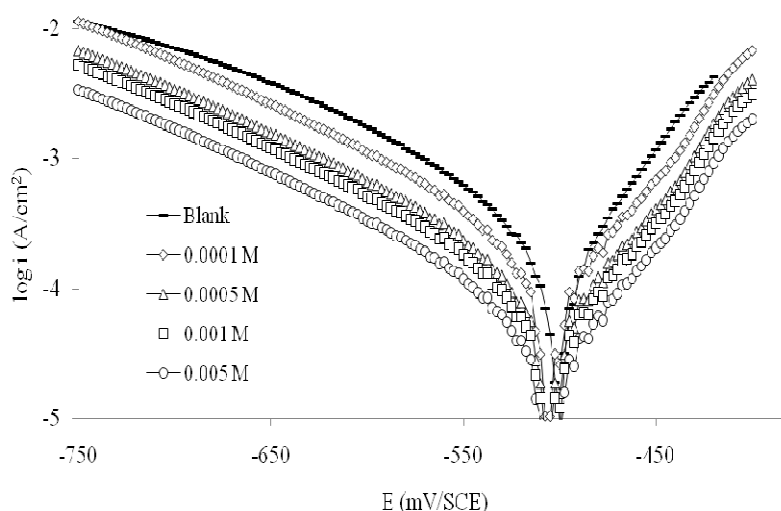


Figure 7. Potentiodynamic polarization curves for iron in $0.5 \text{ M H}_2\text{SO}_4$ containing different concentrations of PPA.

From the experimental values it appears that the addition of the inhibitor decreases the dissolution rate of iron in acid media. The I_{corr} values showed a decrease from 425 to $25 \mu\text{A cm}^{-2}$ on the addition of PPA inhibitor to the acid medium producing an $IE\%$ of 94% .

Data from Table 5 shows that cathodic and anodic Tafel slope values b_a and b_c are almost the same with and without inhibitor, which indicates that the inhibitor adsorbs on metal surface by simply blocking the active sites. The mechanism of anodic and cathodic reactions is not affected. Behaviour of this type has been observed for iron in H_2SO_4 and HCl solutions containing other inhibitors [29,46,47]. The addition of PPA does not alter significantly the value of E_{corr} indicating the mixed type of inhibiting behaviour of the added inhibitor.

Table 5 Polarization parameters and the corresponding inhibition efficiency of iron corrosion in 0.5 M H₂SO₄ containing different concentrations of PPA at 298 K.

C _{inh} (M)	E _{corr} (mV/SCE)	I _{corr} (μA cm ⁻²)	b _a (mV dec ⁻¹)	b _c (mV dec ⁻¹)	EI %
blank	-504.8	425	59	-157.2	-
0.0001	-512.3	240	63.1	140	43
0.0005	-512.3	142	55.4	-140.5	66
0.001	-511.4	55	51	-137.3	87
0.005	-510.6	25	50.2	-1.37	94

3.4. Electrochemical impedance spectroscopy

Electrochemical impedance measurements were carried out the frequency range from 100 kHz to 0.01 Hz at open circuit potential. The Nyquist representations of the impedance of iron in 0.5 M H₂SO₄ with and without addition of various concentrations of PPA are given in Fig. 8. The existence of single semi circle showed the single charge transfer process during dissolution which is unaffected by the presence of inhibitor molecules. Deviation of perfect circular shape is often referred to the frequency dispersion of interfacial impedance. This anomalous behaviour is generally attributed to the inhomogeneity of the metal surface arising from surface roughness or interfacial phenomena [48–50].

The simplest fitting is represented by Randles equivalent circuit (Fig. 9), which is a parallel combination of the charge-transfer resistance (*R_{ct}*) and a constant phase element CPE, both in series with the solution resistance (*R_s*). The impedance of the CPE is expressed :

$$Z_{CPE} = \frac{1}{Y_0(j\omega)^n} \quad (10)$$

where *Y₀* is the magnitude of the CPE, *n* is the exponent (phase shift), ω is the angular frequency and *j* is the imaginary unit. Depending upon the values of *n*, CPE may be resistive for *n* = 0, capacitance for *n* = 1, Warburg impedance for *n* = 0.5 or an inductance for *n* = -1.

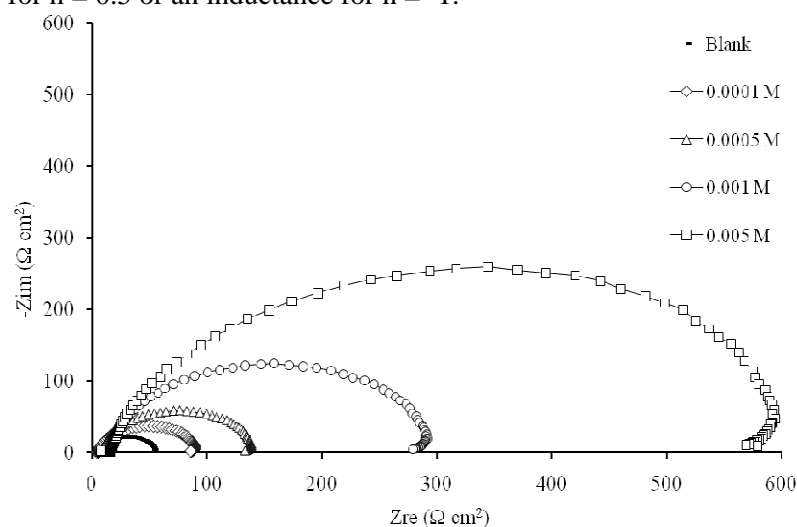


Figure 8 Nyquist plot for iron in 0.5 M H₂SO₄ with and without different concentrations of PPA.

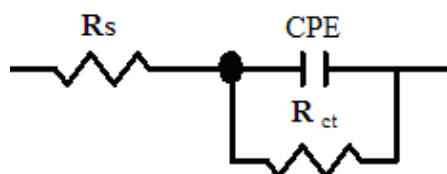


Figure 9 The electrochemical equivalent circuit used to fit the impedance spectra

The charge transfer resistance (R_{ct}) and the constant phase element CPE derived from these curves are given in Table 6. In fact, the addition of inhibitor increases the values of R_{ct} and reduces the CPE. The decrease in CPE is attributed to increase in thickness of electronic double layer [51]. The values of n obtained were close to unity which shows that the interface behaves nearly capacitive. The increase in R_{ct} value is due to the formation of protective film on the metal/solution interface [52,54]. These observations suggest that PPA molecules function by adsorption at metal surface thereby causing the decrease in CPE values and increase in R_{ct} values. The data obtained from EIS technique are in good agreement with those obtained from potentiodynamic polarization and mass loss methods.

Table 6 Electrochemical impedance parameters of iron corrosion in 0.5 M H_2SO_4 containing different concentrations of PPA at 298 K.

C_{inh} (M)	R_s ($\Omega\text{ cm}^2$)	CPE ($\mu\text{F}/\text{cm}^2$)	n	R_{ct} ($\Omega\text{ cm}^2$)	EI%
blank	6	46	0.90	46	-
0.0001	5.25	38.26	0.92	85	44
0.0005	8.06	30.21	0.92	133	65
0.001	7.04	12.05	0.92	284	83
0.005	7.82	5.11	0.93	600	92

3.5. SEM analysis

With the presence of PPA, the film formed is able to protect iron from corrosion according to the results of the electrochemical measurements. In order to further confirm the corrosion resistance ability of the PPA film, scanning electron microscopy was applied to study the surface morphology of Armco iron with and without inhibitor. As can be seen from the Fig. 10, there are distinct differences between the two iron surfaces with and without inhibitor. The SEM photograph Fig. 10(a) shows that the surface is highly damaged in the absence of the inhibitor while Fig. 10(b) shows the formation of a film on the metal surface which causes the corrosion inhibition. The phenomenon implied that the presence of PPA film can protect the Armco iron from corrosion efficiently.

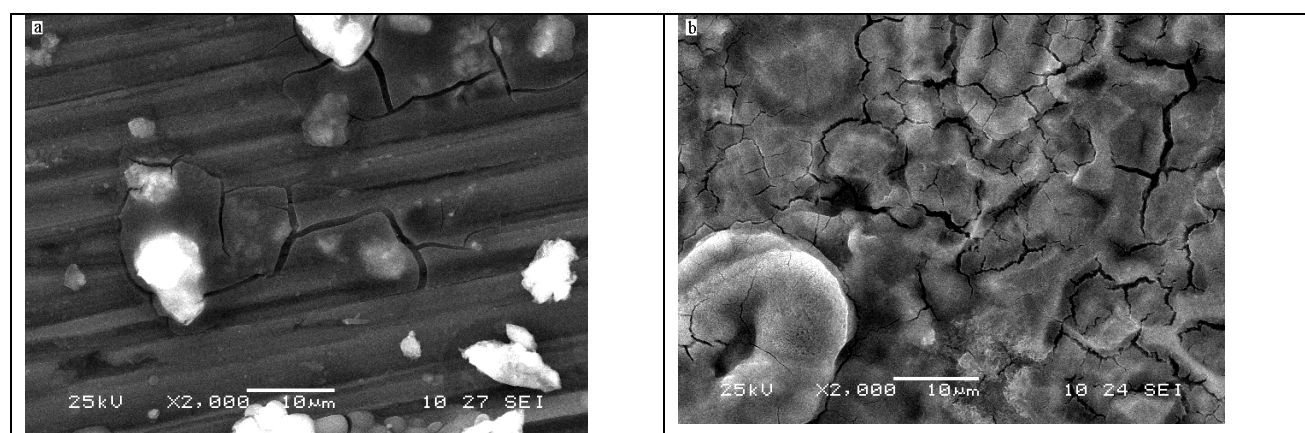


Figure 10 SEM micrographs of samples after immersion in 0.5 M H_2SO_4 (a) without (b) with 5×10^{-3} of PPA.

3.6. Mechanism of inhibition

As follows from weight loss, potentiodynamic polarization and EIS measurements, corrosion of Armco iron in 0.5 M H₂SO₄ is retarded in the presence of different concentrations of PPA. The results clearly showed that the inhibition mechanism involves blocking of iron surface by inhibitor molecules via adsorption. The compound inhibits corrosion by controlling both the anodic and cathodic reactions. In acidic solutions the inhibitor exists as protonated species. These protonated species adsorb on the cathodic sites of iron and decrease the evolution of hydrogen. The adsorption on anodic sites can occur either directly on the basis of donor acceptor interactions between the π electrons of the heterocycle compound and lone pair of electrons of nitrogen and oxygen atom which decrease the anodic dissolution of Armco iron [54].

Conclusion

1. PPA is an efficient inhibitor and the inhibition efficiency increases upon increasing the concentration but decreases upon rising the temperature.
2. The inhibition efficiencies obtained by polarization, EIS and weight loss measurements are in good agreement.
3. Polarization curves show that the inhibitor is a mixed type one.
4. The adsorption of PPA on iron surface was found to be in accordance with Langmuir adsorption isotherm model. From the thermodynamic point of view, the adsorption process is accompanied by a decrease in entropy of the system.
5. The corrosion inhibition potential can be attributed to adsorption which is revealed by SEM studies.

References

1. G. TrabANELLI, *Corrosion* 47 (1991) 410–419.
2. M. Lagrenée, B. Mernari, M. Bouanis, M. Traisnel, F. Bentiss, *Corros. Sci.* 44 (2002) 573–588.
3. S. Kertit, J. Aride, A. Ben-Bachir, A. Sghiri, A. Elkoly, M. Etman, *J. Appl. Electrochem.* 19 (1989) 83–89.
4. L. Wang, *Corros. Sci.* 43 (2001) 1637–1644.
5. M. Abdallah, H.E. Meghed, M. Sobhi, *Mater. Chem. Phys.* 118 (2009) 111–117.
6. X.L. Cheng, H.Y. Ma, S. Chen, R. Yu, X. Chen, Z.M. Yao, *Corros. Sci.* 41 (1999) 321–333.
7. M.A. Hegazy, M. Abdallah, H. Ahmed, *Corros. Sci.* 52 (2010) 2897–2904.
8. S.S. Abd EL-Rehim, M.A.M. Ibrahim, K.F. Khaled, *J. Appl. Electrochem.* 29 (1999) 593–599.
9. V.S. Sastri, *Corrosion Inhibitors: Principles and Applications*, John Wiley & Sons Ltd., New York, 1998.
10. N.S. Ferrara. V. Sez., Suppl. N.8, University of Ferrara, Ferrara, Italy, 1981, p. 453.
11. M.A. Quraishi, I. Ahamad, A.K. Singh, S.K. Shukla, B. Lal, V. Singh, *Mater. Chem. Phys.* 112 (2008) 1035-1039.
12. S.K. Shukla, M.A. Quraishi, *Corros. Sci.* 51 (2009) 1007–1011.
13. G. Moretti, F. Guidi, G. Grion, 2004. *Corros. Sci.* 46, 387-403.
14. A.K. Singh, M.A. Quraishi, *Corros. Sci.* 52 (2010) 152–160.
15. I. Ahamad, M.A. Quraishi, *Corros. Sci.* 52 (2010) 651-656.
16. P. Lowmunkhong, D. Ungthararak, P. Sutthivaiyakit, *Corros. Sci.* 52 (2010) 30-36.
17. I. Obot, I.B., Obi-Egbedi, N.O., *Corros. Sci.* 52 (2010) 282-25.
18. H.S. Awad, S. Turgoose, *Corrosion* 60 (2004) 1168-1179.
19. H. S. Awad, *Anti-Corros. Methods Mater.* 52 (2005) 22-28.
20. J. Jaworska, H.V. Genderen-Takken, A. Hanstveit, E. Plassche, T. Feijtel, *Chemosphere* 47 (2002) 655-665.
21. J.L. Fang, Y. Li, X.R. Ye, Z.W. Wang, Q. Liu, *Corrosion* 49 (1993) 266-271.
22. D.J. Choi, S.J. You, J.G. Kim, *Mater. Sci. Eng. A* 335 (2002) 228-235
23. Y. Gonzalez, M.C. Lafont, N. Pebere, F. Moran, *J. Appl. Electrochem.* 26 (1996) 1259-1265.
24. E.E. Ebenso, *Mater., Chem. Phys.* 71 (2002) 62-70.
25. J. Telegdi, M.M. Shaglouf, A. Shaban, F.H. Karman, I. Betroti, M. Mohai, E. Kalman, *Electrochim. Acta* 46 (2001) 3791-3799.
26. H. Amar, J. Benzakour, A. Derja, D. Villemin, B. Moreau, *J. Electroanal. Chem.* 558 (2003) 131–139.

27. H. Amar, J. Benzakour, A. Derja, D. Villemin, B. Moreau, T. Braisaz, A. Tounsi, *Corros. Sci.* 50 (2008) 124-130.
28. M. R. Laamari, J. Benzakour, F. Berrekhis, A. Abouelfida, A. Derja, D. Villemin, *Arab. J. Chem.* 4 (2011) 271-277.
29. M. R. Laamari, J. Benzakour, F. Berrekhis, A. Derja, D. Villemin, *Les Technologies de Laboratoire.* 5 (2010) 18-25.
30. M. R. Laamari, J. Benzakour, F. Berrekhis, A. Derja, D. Villemin, *Arabian Journal of Chemistry* (2011), doi:10.1016/j.arabjc.2011.03.018
31. M.M. El-Naggar, *Corros. Sci.* 49 (2007) 2226–2236.
32. S.A. Umoren, E.E. Ebenso, *Mater. Chem. Phys.* 106 (2007) 387–393.
33. A.Y. El-Etre, *Corros. Sci.* 45 (2003) 2485–2495.
34. M. Lebrini, F. Bentiss, H. Vezin, M. Lagrenee, *Corros. Sci.* 48 (2006) 1279-1291.
35. M.M. Solomon, S.A. Umoren, I.I. Udosoro, A.P. Udoh, *Corros. Sci.* 52 (4) (2010) 1317–1325.
36. A. Popova, E. Sokolova, S. Raicheva, M. Christov, *Corros. Sci.* 45 (2003) 33-58.
37. S.K. Shukla, M.A. Quraishi, *Corros. Sci.* 51 (2009) 1007–1011.
38. Y. Abboud, A. Abourriche, T. Saffaj, M. Berrada, M. Charrouf, A. Bennamara, H. Hannache, *Desalination*, 237 (2009) 175-189.
39. I.B. Obot, N.O. Obi-Egbedi, *Corros. Sci.* 52 (2010) 198-204
40. I.B. Obot, N.O. Obi-Egbedi, *Colloids Surf. A: Physicochem. Eng. Asp.* 330 (2008) 207- 212.
41. M. Bouklah, B. Hammouti, M. Lagrenee, F. Bentiss, *Corros. Sci.* 48 (2006) 2831-2842.
42. A.K. Singh, M.A. Quraishi, *Corros. Sci.* 53 (2011) 1288–1297.
43. G. Trabanelli, in: F. Mansfeld (Ed.), *Mercel Dekker, New York*, 2006.
44. S.M.A. Hosseini, A. Azimi, *Corros. Sci.* 51 (2009) 728–832.
45. I. Ahamad, R. Prasad, M.A. Quraishi, *Corros. Sci.* 52 (2010) 1472-1481.
46. H. Brandt, M. Fischer, K. Schwabe, *Corros. Sci.* 273 (1979) 273–281.
47. M. Ajmal, A.S. Mideen, M.A. Quraishi, *Corros. Sci.* 36 (1993) 79–84.
48. H. Shih, H. Mansfeld, *Corros. Sci.* 29 (1989) 1235–1240.
49. S. Martinez, M. Metikos-Hukovic, *J. Appl. Electrochem.* 33 (2003) 1137–1142.
50. M. Elayyachy, A. El Idrissi, B. Hammouti, *Corros. Sci.* 48 (2006) 2470–2479.
51. M.G. Hosseini, M. Ehteshamzadeh, T. Shahrabi, *Electrochim. Acta* 52 (2007) 3680-3685.
52. F. Bentiss, M. Traisnel, M. Lagrenee, *Corros. Sci.* 42 (2000) 127–146.
53. S. Murlidharan, K.L.N. Phani, S. Pitchumani, S. Ravichandran, *J. Electrochem. Soc.* 142 (1995) 1478–1483.
54. M.A. Quraishi, J. Rawat, M. Ajmal, *J. Appl. Electrochem.* 30 (2000) 745–751.

(2012) <http://www.jmaterenvironsci.com/>